Water-Dispersible Spherically Hollow Clusters of Magnetic Nanoparticles

Hai-bing Xia,*[,†,‡] Peishan Foo,[§] and Jiabao Yi[⊥]

State Key Laboratory of Crystal Materials, Shandong University, Jinan 250100, P.R. China, Max Planck Institute of Colloids and Interfaces, D-14424 Potsdam, Germany, and Departments of Chemistry and Materials Science and Engineering, National University of Singapore, Singapore 119260

Received January 28, 2009. Revised Manuscript Received March 27, 2009

We reported the synthesis of various water-dispersible clusters of magnetic nanoparticles by self-assembly of a cyclodextrin−polymer surfactant (CD−polymer) complex under one-pot reaction in an aqueous medium. Several polymer surfactants are selected to study their effects on size and morphology of magnetite nanoparticle clusters. They are polyethylene glycol (*n*) nonylphenyl ether series, NPE*n* (where $n = 5, 9, 30$), Brij-97, and Triton X-114. The effect of self-assembly of CD−polymer complexes, which were made up of hydrophilic and hydrophobic groups from the polymer surfactants with CDs, on the cluster formation was also investigated. Depending on the reaction conditions, the structure of the clusters of magnetic nanoparticles can be tuned from mesoporous, to hollow, and to solid by the judicious selection of polymer surfactants. It was also found that an increase in the number of hydrophilic groups of the polymer surfactants caused the size of the Fe_3O_4 nanoparticle clusters to increase. In addition, the self-assembled clusters of the Fe_3O_4 nanoparticle cannot be prepared if the hydrophobic groups of the polymer surfactants cannot be effectively associated with CDs. The Brunauer−Emmett−Teller surface areas and magnetic properties of these nanostructured spherical clusters of Fe_3O_4 nanoparticles were also measured. Other characterizations including Fourier transform infrared, X-ray diffraction, and thermogravimetric analysis were also investigated.

1. Introduction

The challenge in nanoscale science and engineering is currently shifting from *making* new building blocks to *organizing* them into one-, two-, and three-dimensional (1-D, 2-D, and 3-D) structures,[1] which have great potential applications in optical, electronic, magnetic devices, etc. Despite many papers reported on the preparation of 1-D, 2-D, and 3-D crystal architectures, the organization of building blocks into hollow structures have received much attention because of their important applications in many fields.[2−7] The hollow structures with magnetic properties,[8] such as magnetic liposomes[9] and hollow capsules entrapped with magnetic nanoparticles,[10] appear to be a promising technology for targeted drug delivery. The preparation and manipulation of colloid organizations containing magnetic nanoparticles have also attracted special interest for the application in biotechnology and for the study of fundamental phenomena in physics.[11−15] As a result of interparticle interactions, collective properties that affect the magnetic response of these clusters can occur.[16] Therefore, it is desirable to understand and control collective properties of magnetic nanoparticle clusters, which will allow us to produce materials with a highly predictable magnetic response.

The nanoparticle clusters are magnetic and can be manipulated under an external magnetic field. Recently, there

* To whom correspondence should be addressed. E-mail: xia@mpikg.mpg.de; pkuxhb@hotmail.com. Fax: 49 331 5679202.
† Shandong University.
‡ Max Planck Institute of Colloids and Interfaces.
§ Department of Chemistry, National University of Singapore.
⊥ Department of Materials Science and Engineering, National University of Singapore.

(1) Glotzer, S. C.; Solomon, M. J.; Kotov, N. A. *AIChE J.* **2004**, *50*, 2798.
(2) (a) Caruso, F.; Caruso, R. A.; Möhwald, H. *Science* **1998**, *282*, 1111. (b) Göltner, C. G. *Angew. Chem., Int. Ed.* **1999**, *38*, 3155. (c) Caruso, F. *Adv. Mater.* **2001**, *13*, 11.
(3) (a) Dinsmore, A. D.; Hsu, M. F.; Nikolaides, M. G.; Marquez, M.; Bausch, A. R.; Weitz, D. A. *Science* **2002**, *298*, 1006. (b) Noble, P. F.; Cayre, O. J.; Alargova, R. G.; Velev, O. D.; Paunov, V. N. *J. Am. Chem. Soc.* **2004**, *126*, 8092.
(4) (a) Sun, Y.; Xia, Y. *Science* **2002**, *298*, 2176. (b) Sun, Y.; Mayers, B.; Xia, Y. *Adv. Mater.* **2003**, *15*, 641.
(5) Nakashima, T.; Kimizuka, N. *J. Am. Chem. Soc.* **2003**, *125*, 6386.
(6) (a) Yin, Y.; Rioux, R. M.; Erdonmez, C. K.; Hughes, S.; Somorjai, G. A.; Alivisatos, A. P. *Science* **2004**, *304*, 711. (b) Park, S.; Lim, J.-H.; Chung, S.-W.; Mirkin, C. A. *Science* **2004**, *303*, 348.
(7) (a) Goldberger, J.; He, R.; Zhang, Y.; Lee, S.; Yan, H.; Choi, H.-J.; Yang, P. *Nature (London)* **2003**, *422*, 599. (b) Dai, Z. R.; Pan, Z. W.; Wang, Z. L. *J. Am. Chem. Soc.* **2002**, *124*, 8673.
(8) (a) Cao, S.; Zhu, Y.; Ma, M.; Li, L.; Zhang, L. *J. Phys. Chem. C* **2008**, *112*, 1851. (b) Zhao, W.; Chen, H.; Li, Y.; Li, L.; Lang, M.; Shi, J. *Adv. Funct. Mater.* **2008**, *18*, 2780. (c) Hu, P.; Yu, L.; Zuo, A.; Guo, C.; Yuan, F. *J. Phys. Chem. C* **2009**, *113*, 900.
(9) Kuznetsov, A. A.; Filippov, V. I.; Alyautdin, R. N.; Torshina, N. L.; Kuznetsov, O. A. *J. Magn. Magn. Mater.* **2001**, *225*, 95.
(10) Voigt, A.; Buske, N.; Sukhorukov, G. B.; Antipov, A. A.; Leporatti, S.; Lichtenfeld, H.; Bäumler, H.; Donath, E.; Möhwald, H. *J. Magn. Magn. Mater.* **2001**, *225*, 59.
(11) Niemeyer, C. *Angew. Chem., Int. Ed.* **2001**, *40*, 128.
(12) Vestal, C. R.; Zhang, Z. J. *J. Am. Chem. Soc.* **2002**, *124*, 14312.
(13) Tartaj, P.; Serna, C. J. *J. Am. Chem. Soc.* **2003**, *125*, 15754.
(14) Redl, F. X.; Cho, K. S.; Murray, C. B.; O'Brien, S. *Nature (London)* **2003**, *423*, 968.
(15) Rotello, V. M. *Nanoparticles: Building Blocks for Nanotechnology*; Kluwer Academic/Plenum Publishers: New York, 2004.
(16) Allia, P.; Coisson, M.; Tiberto, P.; Viani, F.; Knobel, M.; Novak, M. A.; Nunes, W. C. *Phys. Rev. B: Condens. Matter Mater. Phys.* **2001**, *64*, 144420.

10.1021/cm900268z CCC: $40.75
Published on Web 05/21/2009

has been great interest in magnetic nanoparticles because of their potential applications in many fields,[15,17] such as information storage,[18] ferrofluids,[19] magnetic separation,[20−22] medical diagnosis,[23] and controlled drug delivery.[8,24] Magnetite is by far most commonly employed in biotechnology. However, magnetic nanoparticles have the tendency to agglomerate together once they are formed to reduce the high surface energy of these systems. Hence, controlling the particle size is often difficult. Furthermore, the synthesis of stable clusters of these particles required the clusters formed to be stable and some extent of control on the aggregation of these nanoparticles to form clusters of well-defined shape and size. Thus, the search for facile and flexible synthetic routes is of extreme importance.[25] Furthermore, flexible control of the size of the nanoparticles and clusters will aid in the tuning of their properties for different applications. For instance, in separation processes, the magnetic properties of the loaded nanoparticles can be exploited in their recovery from process streams by using high-gradient magnetic separation (HGMS) technology.[26,27] This process relies on the fact that the force acting on a magnetic particle in a magnetic field depends on the particle size and the magnetic field gradient according to

$$F = -\mu_0 VM\nabla H \quad (1)$$

where V is the volume of the magnetic nanoparticle and M is its magnetization in a given field, H.

HGMS has been examined for the capture of magnetic nanoparticles[21,26−28] where it has been demonstrated, both experimentally and theoretically, that individual nanoparticles cannot be captured effectively by HGMS because diffusion and drag forces can overcome the forces of magnetic attraction to the wires, and the particles are swept through the column relatively unimpeded. Recent studies by Hatton and co-workers[20] also have shown that small clusters of magnetic particles, having a size larger than 50 nm, are more efficient compared to singular nanoparticles because of their high capture efficiency. More recently, extrapolations from the behavior of the bulk material of iron oxide suggest that the critical size for separation is ∼50 nm for the case of an isolated (nonclusterd) particle.[29] This treatment also requires very large applied fields and the latest designs for extremely high gradient separators, both features that make magnetic separations prohibitively expensive in many settings. Therefore, it is necessary to prepare clusters of Fe_3O_4 nanoparticles for their practical applications.

Currently, there are many methods that have been developed to synthesize magnetite clusters.[20] Some of the examples are chemical coprecipitation, polyols, microemulsions, laser pyrolysis, and sol−gel method. Many such coatings have been examined by the Hatton group.[20a] An efficient approach that has gained popularity for synthesizing well-defined clusters is the use of self-assembled structures such as polymers or surfactants.[30] One kind of "magnetomicelles" with the encapsulation of superparamagnetic iron oxide nanoparticles within amphiphilic block-copolymer micelles was synthesized by Taton and co-workers recently.[30d] The magnetic properties of these structures can be controlled by varying the relative concentrations of the magnetic nanoparticles and encapsulating polymer. Yin and co-workers[30f] reported the synthesis of monodisperse magnetite colloidal clusters, which are composed of small primary nanocrystals, by a high-temperature solution-phase process with the use of poly(acrylic acid), PAA. However, most as-prepared clusters were solid aggregates with reduced surface area. Large surface areas per unit volume make the particles ideally suited for use in drug delivery[8a] and adsorptive separations[21,26] since their capacity for targeted solutes is considerably greater than the capacity of commercial resins.

The use of intermolecular interactions to control the type and shape of the clusters were possible as suggested by many reports.[31] Rotello and co-workers[32] reported that polymeric monolayer-protected gold particles self-assembled into spherical aggregates through hydrogen-bonding interactions. In their strategy, the polymers acted as the mortar to hold the colloidal particles together to form spherical aggregates. It was shown that hydrogen bonding aided in the formation of spherical clusters while the absence of hydrogen bonding demonstrated the lack of aggregation. Jiang and co-workers reported a strategy directed by $\pi-\pi$ interactions for the self-assembly of individual magnetic nanoparticles into structured ensembles.[30a] The hydroxyl groups from cyclodextrins (CDs)

(17) Sun, S.; Anders, S.; Hamann, H. F.; Thiele, J.; Baglin, J. E.; Thomson, T.; Fullerton, E. E.; Murray, C. B.; Terris, B. D. *J. Am. Chem. Soc.* **2002**, *124*, 2884.
(18) Schmid, G., Ed. *Nanoparticles: From Theory to Application*; John Wiley & Sons: New York, 2004.
(19) Klokkenburg, M.; Vonk, C.; Claesson, E. M.; Meeldijk, J. D.; Erne, B. H.; Philipse, A. P. *J. Am. Chem. Soc.* **2004**, *126*, 16706.
(20) (a) Ditsch, A.; Laibinis, P. E.; Wang, I. C.; Hatton, T. A. *Langmuir* **2005**, *21*, 6006. (b) Cannas, C.; Ardu, A.; Musinu, A.; Peddis, D.; Piccaluga, G. *Chem. Mater.* **2008**, *20*, 6364.
(21) Moeser, G. D.; Roach, K. A.; Green, W. H.; Hatton, T. A. *AIChE J.* **2004**, *50*, 2835.
(22) Ditsch, A.; Lindenmann, S.; Laibinis, P. E.; Wang, D. L. C.; Hatton, T. A. *Ind. Eng. Chem. Res.* **2005**, *44*, 6824.
(23) Megens, M.; Prins, M. *J. Magn. Magn. Mater.* **2005**, *293*, 702.
(24) Tang, B. Z.; Geng, Y.; Lam, J. W. Y.; Li, B.; Jing, X.; Wang, X.; Wang, F.; Pakhomov, A. B.; Zhang, X. X. *Chem. Mater.* **1999**, *11*, 1581.
(25) (a) Tartaj, P.; González-Carreño, T.; Serna, C. J. *Adv. Mater.* **2004**, *16*, 529. (b) Tartaj, P.; Morales, M. P.; González-Carreño, T.; Veintemillas-Verdaguer, S.; Serna, C. J. *J. Magn. Magn. Mater.* **2005**, *290−291*, 28.
(26) Moeser, G. D.; Roach, K. A.; Green, W. H.; Laibinis, P. E.; Hatton, T. A. *Ind. Eng. Chem. Res.* **2002**, *41*, 4739.
(27) Bucak, S.; Jones, D. A.; Laibinis, P. E.; Hatton, T. A. *Biotechnol. Prog.* **2003**, *19*, 477.
(28) (a) Fletcher, D. *IEEE Trans. Magn.* **1991**, *27*, 3655. (b) Gerber, R.; Takayasu, M.; Friedlaender, F. J. *IEEE Trans. Magn.* **1983**, *19*, 2115.
(29) Yavuz, C. T.; Mayo, J. T.; Yu, W. W.; Prakash, A.; Falkner, J. C.; Yean, S.; Cong, L.; Shipley, H. J.; Kan, A.; Tomson, M.; Natelson, D.; Colvin, V. L. *Science* **2006**, *214*, 964.
(30) (a) Jin, J.; Iyoda, T.; Cao, C.; Song, Y.; Jiang, L.; Li, T.; Zhu, D. *Angew. Chem., Int. Ed.* **2001**, *40*, 2135. (b) Bonnemann, H.; Nagabhushana, K. S. *Nanotechnol. Catal.* **2004**, *1*, 51. (c) Deng, H.; Li, X.; Peng, Q.; Wang, X.; Chen, J.; Li, Y. *Angew. Chem., Int. Ed.* **2005**, *44*, 2782. (d) Kim, B. S.; Qiu, J. M.; Wang, J. P.; Taton, T. A. *Nano Lett.* **2005**, *5*, 1987. (e) Bai, F.; Wang, D.; Huo, Z.; Chen, W.; Liu, L.; Liang, X.; Chen, C.; Wang, X.; Peng, Q.; Li, Y. *Angew. Chem., Int. Ed.* **2007**, *46*, 6650. (f) Ge, J.; Hu, Y.; Biasini, M.; Beyermann, W. P.; Yin, Y. *Angew. Chem., Int. Ed.* **2007**, *46*, 4342.
(31) (a) Liu, J.; Alvarez, J.; Kaifer, A. E. *Adv. Mater.* **2000**, *12*, 1381. (b) Ikari, K.; Suzuki, K.; Imai, H. *Langmuir* **2006**, *22*, 802.
(32) (a) Boal, A. K.; Ilhan, F.; Derouchey, J. E.; Thurn-Albrecht, T.; Russell, T. P.; Rotello, V. M. *Nature (London)* **2000**, *404*, 746. (b) Carroll, J. B.; Frankamp, B. L.; Rotello, V. M. *Chem. Commun.* **2002**, *17*, 1892.

have strong adsorption capacity with the surface of Fe_3O_4 nanoparticles, rendering them water-soluble. Yang and coworkers have demonstrated that hydrophobic Fe_3O_4 nanoparticles were transferred into aqueous solution, in which Fe_3O_4 nanoparticles were stabilized by the CDs.[33]

It is well-known that CDs form mainly a 1:1 complex with the hydrophobic part of the surfactants when the aliphatic chains length is smaller than that of C_{10}.[34] Moreover, the experimental results were also demonstrated that there are two ethylene oxide units for each CD molecule when the CD−polymer complexes are formed.[35] Therefore, self-assembly of a CD−polymer complex has an effect on the cluster formation of Fe_3O_4 nanoparticles. In our previous work,[36] water-dispersible Fe_3O_4 clusters were prepared by use of the polymer surfactant polyethylene glycol (5) nonylphenyl ether (NPE_5) and cyclodextrins. The self-assembled structures of water-dispersible magnetite clusters can be formed in a one-pot reaction under mild conditions in an aqueous medium. These mesoporous, spherical magnetic clusters of Fe_3O_4 nanoparticles possessed a Brunauer−Emmett−Teller (BET) surface area of ca. 141.1 $m^2\ g^{-1}$, which is very important for them as magnetic carriers. After the formation of an inclusion complex with the hydrophobic groups of the surfactant NPE_5, the hydroxyl groups of the α-CD rims can interact with the hydrophilic moiety of the surfactant and among CDs.[36,37] This would result in the possible formation of hydrogen bonding among CDs and between the surfactant NPE_5 and CDs. As the number of hydrophilic groups of the surfactant and CD concentration increase, it was likely that these interactions among them would increase. This might lead to linkage or bridging of the surface coating on the nanoparticles and further enhance the interactions between singular nanoparticles, causing them to be bound together. Herein, it is desirable to study the effect of self-assembly of a CD−polymer complex on the morphology of Fe_3O_4 nanoparticle clusters. Several polymeric surfactants are selected to study their effects on particle size and morphology of the water-soluble magnetite clusters. They are polyethylene glycol (*n*) nonylphenyl ether series, NPE*n* (where $n = 5, 9, 30$), Brij-97, and Triton X-114. The effect of hydrophilic and hydrophobic groups from the polymer surfactants on the cluster formation by self-assembly was also investigated. Depending on the reaction conditions, the structure of the clusters of magnetic nanoparticles can tuned from mesoporous, to hollow, and to solid by the judicious selection of polymer surfactants. It was also found that an increase in the number of hydrophilic groups of the surfactants caused the size of the Fe_3O_4 clusters to increase. In addition, the self-assembled clusters cannot be prepared if the hydrophobic groups of the surfactants cannot be effectively associated with CD. The BET surface areas and magnetic properties of these nanostructured spherical clusters were also measured. Other characterizations including Fourier transform infrared (FTIR) spectroscopy, X-ray diffraction (XRD), and thermogravimetric analysis (TGA) were also investigated.

Scheme 1. Molecular Structure of the NPE*n* Series, Brij-97, Triton X-114, and cyclodextrin

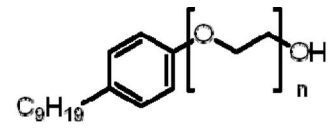

n=5, 9, and 30 for NPE_5, NPE_9 and NPE_{30}, respectively.

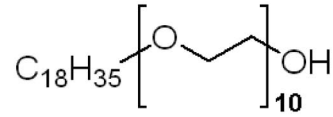

Brij® 97

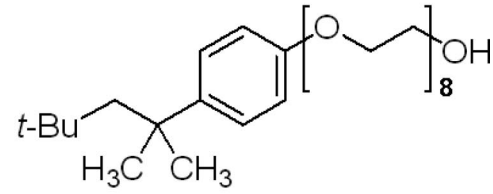

Triton® X-114

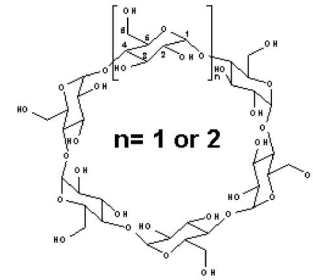

Cyclodextrin

2. Experimental Section

Materials. Chemicals such as the NPE*n* series (polyethylene glycol (*n*) nonylphenyl ether, 4-$(C_9H_{19})C_6H_4(OCH_2CH_2)_nOH$, $n \sim 5, 9, 30$), Brij-97 (polyoxyethylene (10) oleyl ether, $C_{18}H_{35}(OCH_2CH_2)_nOH$, $n \sim 10$), Triton X-114 (polyoxyethylene (8) isooctylphenyl ether, 4-$(C_8H_{17})C_6H_4(OCH_2CH_2)_nOH$, $n \sim 8$), α- and β-CD (cyclodextrin), ferric(II) chloride with tetrahydrate ($FeCl_2 \cdot 4H_2O$), and anhydrous ferric(III) chloride ($FeCl_3$) were used without further purification (Scheme 1).

Synthesis of Hollow Clusters of Fe_3O_4 Nanoparticles. NPE_9 (1.965 g, 5% solution w/w, 2.62 mmol) was dissolved in 45 mL of deoxygenated water with vigorous stirring and under nitrogen gas. $FeCl_2 \cdot 4H_2O$ (0.158 g, 0.79 mmol) and $FeCl_3$ (0.258 g, 1.54 mmol) were then added to the solution. After about 30 min of stirring, 1.2 mL of $NH_3 \cdot H_2O$ (28%, w/w) in 30 mL of 5 mM α-CD solution was added when there was no powder in the mixture solution. The reaction was allowed to further proceed for another 1.5 h with constant and vigorous stirring to produce a water-based suspension. Nitrogen gas was continuously purged during the whole experiment process. Different concentrations of NPE_9 from 0.215 to 3.5 mM

(33) Wang, Y.; Wong, J. F.; Teng, X.; Lin, X. Z.; Yang, H. *Nano Lett.* **2003**, *11*, 1555.
(34) Saint Aman, E.; Serve, D. *J. Colloid Interface Sci.* **1990**, *138*, 365.
(35) Topchieva, I.; Karezin, K. *J. Colloid Interface Sci.* **1999**, *213*, 29.
(36) Xia, H.; Yi, J.; Foo, P.; Liu, B. *Chem. Mater.* **2007**, *19*, 4087.
(37) Cunha-Silva, L.; Teixeira-Dias, J. J. C. *J. Phys. Chem. B* **2002**, *106*, 3323.

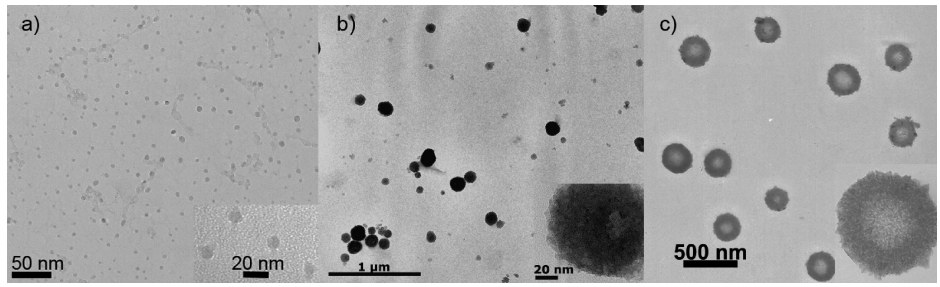

Figure 1. TEM images of Fe_3O_4 clusters at (a) $[NPE_5] = 0.75$ mM, (b) $[NPE_5] = 6$ mM, and (c) $[NPE_9] = 1.75$ mM ($[\alpha\text{-CD}] = 2$ mM, $[Fe^{2+}] = 10$ mM, $[Fe^{3+}] = 20$ mM).

(under fixed other reaction conditions) were also conducted to investigate their effect on the morphology of formed clusters.

A similar synthesis procedure was conducted except that the NPE_9 was replaced by other surfactants. The as-prepared sample solution was rather stable in aqueous solution. However, high-speed centrifugation and ultrasonication longer than 10 min would destroy the spherical structure.

Characterization. The size and morphology of the Fe_3O_4 nanoparticles were examined by transmission electron microscopy (TEM) using a JSM-2010F microscope. Ten microliters of as-prepared original sample solution was extracted and dropped onto the copper grids with carbon coating. The structure of the powder samples was determined by XRD using a Siemens D5005 diffractometer equipped with a Cu Kα (1.5405 Å) X-ray source. The molecular structure of the samples was further determined by FTIR spectroscopy using KBr platelets with FTS 3000, Bio-Rad Excalibur Series. The thermogravimetric analysis was carried out with a TGA 2960 double beam using a heating rate of 20 °C/min in air. Magnetic property of the hollow cluster of magnetic nanoparticles was conducted by using a superconducting quantum interference device magnetometer. Before the characterization of XRD, FTIR, TGA, and magnetic property, the as-prepared sample was dried at 60 °C for 12 h under nitrogen protection.

3. Results and Discussion

3.1. Effect of CD−Polymer Complex on the Morphology of Fe_3O_4 Nanoparticle Clusters. TEM images of dispersed and clustered Fe_3O_4 nanoparticles are shown in Figure 1. Uniform Fe_3O_4 nanoparticles with an inner diameter of about 10 nm are obtained (Figure 1a) when $[NPE_5]$ is at 0.75 mM and [CD] is 2 mM (the concentration of NPE_5 represented as $[NPE_5]$). These nanoparticles are well-separated because of the coating on their surface, reducing their tendency to agglomerate by steric repulsive forces. Furthermore, distinct spherical Fe_3O_4 nanoparticle aggregates are formed with a diameter of 80−120 nm (Figure 1b) when $[NPE_5]$ is at 6 mM and [CD] is 2 mM. Different morphology is obtained when the NPE_5 is replaced by NPE_9, even if the same [CD] is kept. Hollow spherical clusters of size close to 300 ± 50 nm are formed. The thickness of the shell is about 58 nm with a center of around 170 nm (Figure 1c). Therefore, different types of clusters of Fe_3O_4 nanopartilces can be obtained by controlling the concentrations of NPE*n* and CD. This is because the different CD−polymer complexes will be formed when $[NPE_n]$ is changed. Several polymeric surfactants are selected to study the effect of self-assembly of CD−polymer complexes on the morphology of Fe_3O_4 nanoparticle clusters. They are polyethylene glycol (*n*) nonylphenyl ether series, NPE*n* (where $n = 5$, 9, 30), Brij-97, and Triton X-114. To investigate the effect of the number of hydrophilic groups from the polymer surfactants on the Fe_3O_4 clusters formed, NPE_5, NPE_9, and NPE_{30} were used (Scheme 1). As the surfactant used was changed from NPE_5 to NPE_9 and then to NPE_{30}, the number of hydrophilic groups changed from 5 to 9 and then to 30, respectively. In a comparison of the Fe_3O_4 nanoparticle clusters formed from using the different polymer surfactants, the effect of the change in the number of hydrophilic groups can be observed. In addition, the effect of hydrophobic groups of the polymer surfactants on the clusters formed was also investigated. In a comparison of the results from Triton X-114 and Brij-97 to those from NPE_9, the effect can be clearly shown. Triton X-114 and Brij-97 have approximately the same number of hydrophilic groups as NPE_9 but the types of hydrophobic groups differ. For NPE_9, the hydrophobic groups consist of a straight C_9 chain, *n*-nonyl, attached to a phenyl group. Triton X-114 has a structure similar to that of NPE_9 except that the group attached to the phenyl group is *tert*-octyl. The hydrophobic moiety of Brij-97 consists of an aliphatic straight chain of C_{18} without any phenyl group present (Scheme 1).

3.2. Effect of NPE_9 Concentration on Morphology of Fe_3O_4 Nanoparticle Clusters. The effect of NPE_9 concentration (represented by $[NPE_9]$) on the size and morphology of Fe_3O_4 nanoparticles clusters was investigated. Previous work suggested that the coated Fe_3O_4 nanoparticles do not cluster in the presence of a low concentration of surfactant.[20] Thus $[NPE_9]$ was varied from 0.215 o 3.50 mM. The TEM images of several concentrations of NPE_9 used were shown in Figure 2. Because of the electron loosening of the surfactant and the thin layer of the coating, only the cores of Fe_3O_4 nanoparticles could be seen in the micrograph (Figure 2a) when $[NPE_9]$ was 0.215 mM. When $[NPE_9]$ was 0.875 mM, irregular clusters of average size around 44 nm were formed (Figure 2b). At 2.15 mM, the main product formed was dense spherical clusters about 270 nm in diameter (Figure 2c). Increasing the concentration further resulted in the formation of irregular clusters of Fe_3O_4 nanoparticles (Figure 2d).[38] The results show that as the concentration increased from 0.215 to 1.75 mM, there was an increase in the amount of Fe_3O_4 clusters formed. These clusters were also more regular and larger in size. However, after $[NPE_9]$ was over 1.75 mM, the amount and size of spherical clusters decreased. The $[NPE_9]$ plays a key role in the type and size of spherical Fe_3O_4 clusters obtained.

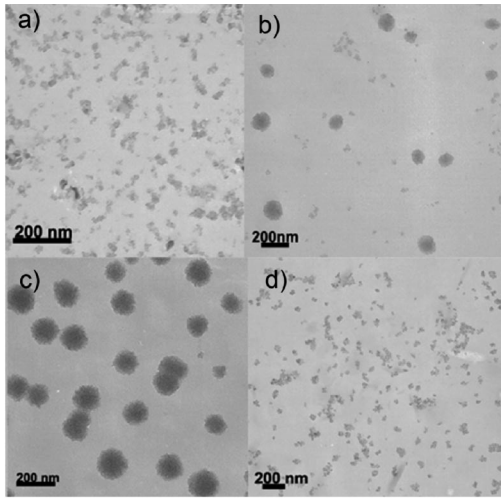

Figure 2. TEM images of Fe_3O_4 clusters at different [NPE_9]: (a) 0.215 mM, (b) 0.875 mM (c) 2.15 mM, and (d) 3.50 mM ([α-CD] = 2 mM, [Fe^{2+}] = 10 mM, [Fe^{3+}] = 20 mM).

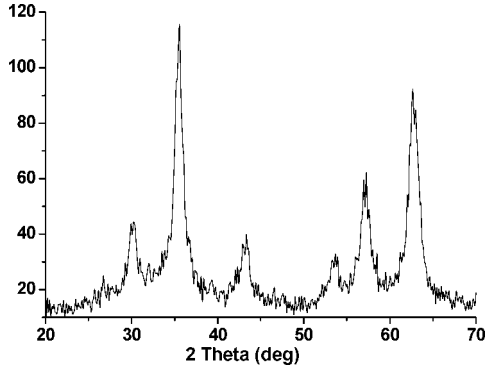

Figure 3. XRD pattern of magnetite product ([α-CD] = 2 mM, [NPE_9] = 1.75 mM, [Fe^{2+}] = 10 mM, [Fe^{3+}] = 20 mM).

3.3. X-ray Diffraction. The diffraction pattern (Figure 3) was consistent with the standard Fe_3O_4 reflection, confirming the nanoparticles formed were Fe_3O_4.[36] The Fe_3O_4 nanoparticles display several relatively strong reflection peaks in the 2θ region of 20°−70°, which is similar to those of the Fe_3O_4 nanoparticles reported by other groups, confirming that the nanoparticles prepared are Fe_3O_4. These strong Bragg reflections of Fe_3O_4 are at the 2θ angles of 30.1° (d = 2.967 Å), 35.4° (d = 2.532 Å), 43.0° (d = 2.101 Å), 53.4° (d = 1.714 Å), 56.9° (d = 1.616 Å), and 62.5° (d = 1.484 Å). These corresponded to the indices (220), (311), (400), (422), (511), and (440) respectively.[30,36,44]

The average diameters of the singular Fe_3O_4 nanocrystals (D) could be estimated by line broadening using the Scherrer equation

$$D = K\lambda/(\beta \cos \theta) \quad (2)$$

where K is a constant approximately equal to unity and related to several aspects including the shape of the crystal and the Miller index of the reflecting crystallographic planes and crystallite shape, β is the angular width in radians at half-maximum intensity, and θ is the Bragg angle.[45] K is often assigned as 0.89.[46,47] The estimated D value associated with the strongest (311) reflection of the Fe_3O_4 at 2θ = 35.3° was about 9 nm, which was in good agreement with the average size of singular nanoparticles observed from TEM, allowing for experimental errors.

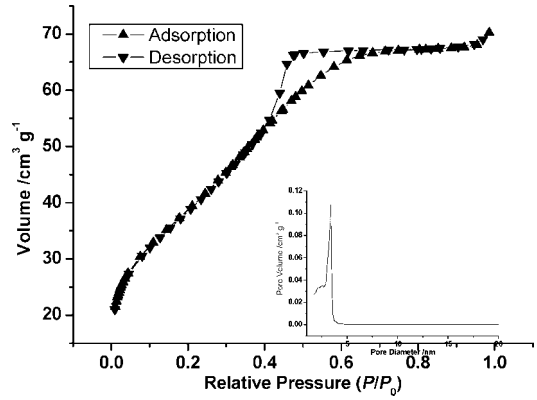

Figure 4. Nitrogen adsorption−desorption isotherm of the obtained hollow clusters of magnetite nanoparticles measured at 77 K; inset shows pore diameter distribution of the sample ([α-CD] = 2 mM, [NPE_9] = 1.75 mM, [Fe^{2+}] = 10 mM, [Fe^{3+}] = 20 mM).

3.4. BET Surface Area. The isothermal N_2 sorption data of Fe_3O_4−NPE_9 with α-CD at 77 K are shown in Figure 4. Quantitative calculation indicates that the hollow clusters of Fe_3O_4 nanoparticles possess a BET surface area of ca.141.2 $m^2\ g^{-1}$ with a diameter of 300 nm and narrows a distribution of pore diameter centered at 3.4 nm (Figure 4, inset). Compared with our previous result[36] (Fe_3O_4−NPE_5 with α-CD), the clusters of Fe_3O_4−NPE_9 with α-CD have a narrow pore distribution and are more porous because of the hollow cores, which is indicated by the sharp increase at low P/P_0 in the curve. The magnetic clusters of sufficiently high specific surface area[51] can be used in the separation of target molecules from a multiphase complex system by external magnetic devices and would have high load capacity of target molecules. The as-synthesized hollow clusters of the magnetic nanoparticles do not compromise the surface area (ca. 141.2 $m^2\ g^{-1}$ with a diameter of 300 nm), determining adsorptive capacity as separated Fe_3O_4 nanoparticles with coating have a BET surface area of ca. 164.6

(38) Prozorov, T.; Kataby, G.; Prozorov, R.; Gedanken, A. *Thin Solid Films* **1999**, *340*, 189.
(39) Sugimoto, T. *Monodispersed Particles*; Elsevier Science B.V.: The Netherlands, 2001.
(40) Qiao, R.; Zhang, X. L.; Qiu, R.; Kim, J. C.; Kang, Y. S. *Chem. Mater.* **2007**, *19*, 6485.
(41) Du, X.; Chen, X.; Lu, W.; Hou, J. *J. Colloid Interface Sci.* **2004**, *274*, 645.
(42) Datta, A.; Mandal, D.; Pal, S. K.; Das, S.; Bhattacharyya, K. *J. Chem. Soc., Faraday Trans.* **1998**, *94*, 3471.
(43) Buschmann, H. J.; Jansen, K.; Schollmeyer, E. *J. Inclusion Phenom.* **2000**, *37*, 231.
(44) Cornell, R. M.; Schwertmann, U. *The Iron Oxides: Structure, Properties, Reactions, Occurrence and Uses*; VCH Publishers: New York, 1996.
(45) Klug, H. P.; Alexander, L. E. *X-Ray Diffraction Procedures for Polycrystalline and Amorphous Materials*; John Wiley & Sons, Inc.: New York, 1954.
(46) Pouget, J. P.; Jozefowicz, M. E.; Epstein, A. J.; Tang, X.; MacDiarmid, A. G. *Macromolecules* **1991**, *24*, 779.
(47) Moon, Y. B.; Cao, Y.; Smith, P.; Heeger, A. *J. Polym. Commun.* **1989**, *30*, 196.
(48) Tang, B. Z.; Geng, Y.; Lam, J. W.; Li, B.; Jing, X.; Wang, X.; Wang, F.; Pakhomov, A. B.; Zhang, X. X. *Chem. Mater.* **1999**, *11*, 1581.
(49) Lellouche, J. P.; Senthil, G.; Joseph, A.; Buzhansky, L.; Bruce, I.; Bauminger, E. R.; Schlesinger, J. *J. Am. Chem. Soc.* **2005**, *127*, 11998.
(50) Shen, L.; Laibinis, P. E.; Hatton, T. A. *Langmuir* **1999**, *15*, 447.
(51) Wu, P. G.; Zhu, J. H.; Xu, Z. H. *Adv. Funct. Mater.* **2004**, *14*, 345.

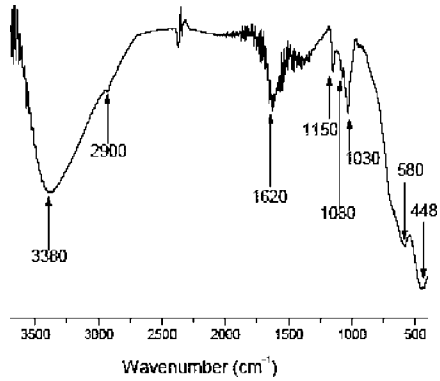

Figure 5. FTIR spectrum of the obtained hollow cluster of magnetite nanoparticles ([α-CD] = 2 mM, [NPE_9] = 1.75 mM, [Fe^{2+}] = 10 mM, [Fe^{3+}] = 20 mM).

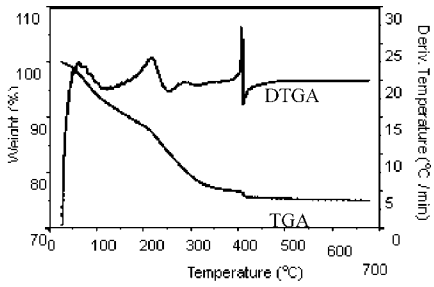

Figure 6. TGA curve of obtained hollow clusters of magnetite nanoparticles ([α-CD] = 2 mM, [NPE_9] = 1.75 mM, [Fe^{2+}] = 10 mM, [Fe^{3+}] = 20 mM).

m^2 g^{-1} with a diameter of 10 nm (Table S1, Supporting Information).

3.5. FTIR Spectrum. In the FTIR spectrum of the as-prepared product (Figure 5), the peaks at 580 and 448 cm^{-1} indicate the presence of magnetite. These peaks corresponded to the symmetric Fe−O stretch and antisymmetric Fe−O vibration, respectively.[52] The broad band at about 3380 cm^{-1} was due to the OH stretching, which was contributed by the OH groups in both NPE_9 and CD. The small peak around 2900 cm^{-1} was due to the stretching vibrations of CH_2 and CH_3 of the alkyl groups on NPE_9. The peaks in the region 1000−2000 cm^{-1} should be attributed to both CD and NPE_9 vibrations. The strong band at about 1150 cm^{-1} corresponded to the C−O−C vibration and the bands at about 1080 and 1030 cm^{-1} arose from the coupled stretch vibration of C−C and C−O. The peak at about 1620 cm^{-1} was due to the CH_2 bending vibration. Hence, from the FTIR spectrum, the magnetite nanoparticles were formed and were coated with both NPE_9 and CD.

3.6. Thermogravimetric Analysis (TGA). Figure 6 shows the TGA analysis curves of as-prepared product. There were three obvious weight losses in the DTGA curve. The initial weight loss from room temperature to 125 °C was attributed to the loss of surface-adsorbed water. The second weight loss over the temperature range of 125−256 °C was most probably due to the release of the CDs attached to the particles. The smaller weight loss later in the temperature range of 256−310 °C was due to the evaporation of NPE_9

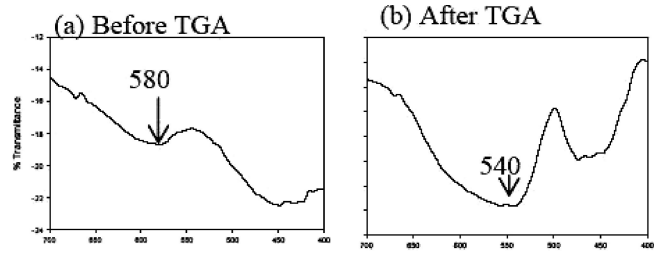

Figure 7. FTIR spectra of obtained hollow clusters of magnetite nanoparticles before and after TGA ([α-CD] = 2 mM, [NPE_9] = 1.75 mM, [Fe^{2+}] = 10 mM, [Fe^{3+}] = 20 mM).

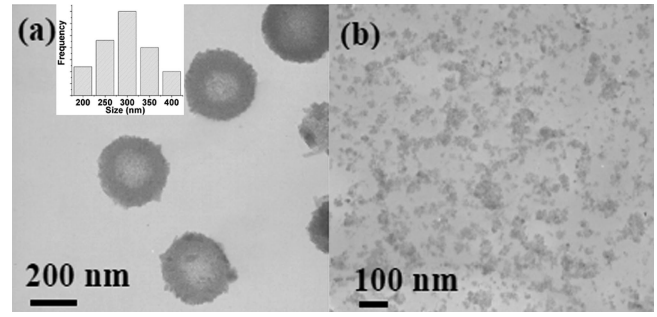

Figure 8. TEM images of Fe_3O_4 clusters at different [α-CD]: (a) 2.5 mM and (b) 7.5 mM ([NPE_9] = 1.75 mM, [Fe^{2+}] = 10 mM, [Fe^{3+}] = 20 mM). Inset shows a histogram of the size distribution of the clusters.

attached to the particles.[53] From the graph, the weight percentage of the layer of coating was about 13.7%. The percentage weight of the NPE_9 and CD was 5.26% and 8.42%, respectively. Converting these values to mole ratio, the stoichiometric ratio of the complex of NPE_9 and CD was found to be about 1:1. After heating, about 75% of the iron oxide powder was still present. The color of the solid retrieved after the TGA was red, indicating a change in the form of magnetite. This was due to the oxidation of magnetite particles. Magnetite is oxidized to maghemite (γ-Fe_2O_3) below 100 °C in air and then at temperatures above 300 °C maghemite undergoes a structural phase transition to hematite (α-Fe_2O_3). To confirm the structure of the solid after TGA, FTIR spectroscopy was carried out on the solid. The FTIR spectra of the solid from before and after the TGA (Figure 7) showed that the peak from 580 cm^{-1} shifted to 540 cm^{-1}, confirming the change of magnetite to hematite.[44,54] Hence, the sharp change at 409 °C in the DTGA curve was most likely due to the rapid transformation of maghemite to hematite.

3.7. Effect of α-CD Concentration. The TEM images of the clusters of Fe_3O_4 nanoparticles using different concentrations of α-CD at fixed concentration of NPE_9 are shown in Figure 8. When the concentration of CD was within the range of 1−2 mM, the morphology of the clusters of Fe_3O_4 nanoparticles was almost identical (300 ± 50 nm, inset shows a histogram of the size distribution of the clusters). Increasing the concentration of α-CD to 3 mM, small, dispersed, and irregular nanoparticle clusters were formed.

3.8. Effect of *β*-CD. The CDs were absorbed on the surfaces of Fe_3O_4 nanoparticles. The different types of CDs

(52) Bruce, I. J.; Taylor, J.; Todd, M.; Davies, M. J.; Borioni, E.; Sangregorio, C.; Sen, T. *J. Magn. Magn. Mater.* **2004**, *284*, 145.
(53) Hou, Y.; Kondoh, H.; Shimojo, M.; Sako, E. O.; Ozaki, N.; Kogure, T.; Ohta, T. *J. Phys. Chem. B* **2005**, *109*, 4845.
(54) Chamritski, I.; Burns, G. *J. Phys. Chem. B* **2005**, *109*, 4965.

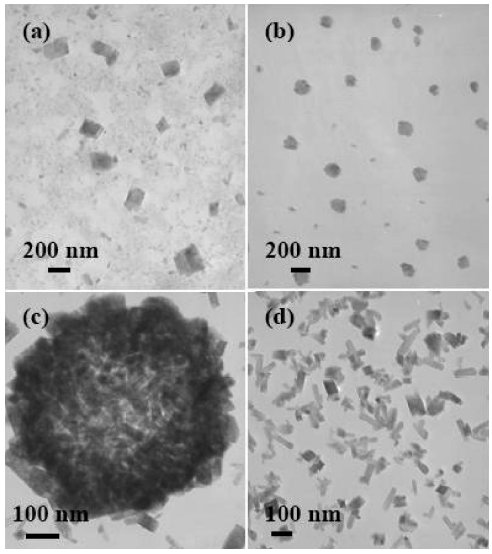

Figure 9. TEM images of Fe_3O_4 clusters at different [NPE_9]: (a) 0.215 mM, (b) 1.75 mM, (c) 2.15 mM, and (d) 3.50 mM ([β-CD] = 2 mM, [Fe^{2+}] = 10 mM, [Fe^{3+}] = 20 mM).

have different adsorption capacities on the crystal plane of the nuclei of Fe_3O_4 nanoparticles formed at the initial stage, additionally having an effect on the morphology of the formed Fe_3O_4 nanoparticles. In addition, considering the cost of α-CD, β-CD is more economical. Hence, the feasibility of substituting α-CD with β-CD and the effect of CD type were investigated. The TEM images of the Fe_3O_4 nanoparticle clusters formed using 2 mM β-CD with different concentrations of NPE_9 are shown in Figure 9. When [NPE_9] was 0.21 mM, a mixture of small, irregular nanoparticles and cubic structure clusters were formed. As the concentration increased to 2.15 mM, spherical hollow clusters were formed, similar to the ones formed using α-CD. The size of the clusters was 667 nm, which was much bigger than the size of the clusters formed using α-CD. The particles that made up the clusters were cubic-type particles, unlike the small spherical-type nanoparticles that made up the clusters formed using α-CD. At 3.5 mM, a mixture of cubic particles and rods was observed. Hence, changing the type of CD will affect the morphology of the nanoparticles and the size of the clusters. Furthermore, it was observed that the same type of clusters could be obtained using both types of CD.

The difference in the morphology observed when different types of CD were used should be due to the difference in the size of the cavity and the number of hydroxyl groups in the rim. β-CD has a larger cavity than α-CD and also one more glucopyranose unit. It is possible that two surfactant molecules can be complexed into one cavity of β-CD.[34] Hence, even though an inclusion complex was formed in both cases, there was still a difference in the complex formed. The α-CD and β-CD have different adsorption capacities on the nuclei and caused differentiated growth rates in certain directions.[39] This may favor the formation of the cubic nanoparticles instead of spherical-type particles when β-CD was used.

3.9. Magnetic Property. When the field was cycled between −50 and 50 kOe, the saturated magnetization curve

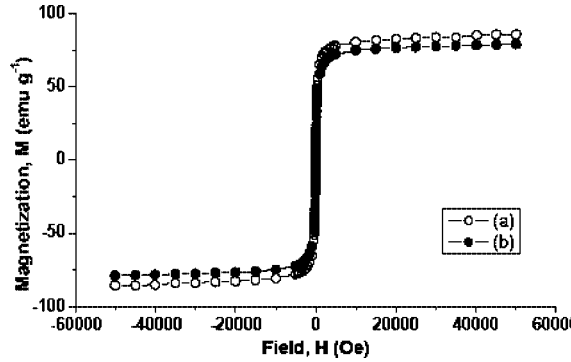

Figure 10. Room-temperature magnetization curves of obtained hollow clusters of magnetite nanoparticles using (a) 2 mM α-CD and (b) 2 mM β-CD ([NPE_9] = 1.75 mM, [Fe^{2+}] = 10 mM, [Fe^{3+}] = 20 mM).

of the Fe_3O_4 nanocrystals with α-CD and β-CD obtained at 300 K was consistent with superparamagnetic characteristics (Figure 10).[36,48] The saturation magnetization value of as-prepared hollow clusters of Fe_3O_4 nanocrystals is 85.7 emu g^{-1} for α-CD and 79 emu g^{-1} for β-CD from the magnetization curves, respectively. The real value should be 114.3 emu g^{-1} for α-CD and 105.3 emu g^{-1} for β-CD because the weight ratio of Fe_3O_4 in the hollow structures is about 75% according to TGA results. The value was still lower than that of bulk bare magnetite (∼130 emu g^{-1})[49] but were comparable to that of the coated magnetite synthesized in other reports (∼87 emu g^{-1}).[50] The observed lower values compared to those of the bare magnetite might be caused by low crystalline quality of magnetite or the surface spin-canting effects or the surfactant coating which might reduce the total magnetic moment of the nanoparticles, which resulted in a decreased magnetization.[36,48]

Substituting α-CD with β-CD resulted in an increase in cluster size but the magnetization of the magnetite clusters was very close. Therefore, in circumstances in which the size of the clusters would not pose a problem, magnetite clusters synthesized by β-CD could be used. However, the solubility of β-CD is much lower compared to that of α-CD and, hence, at higher concentrations of CD, the synthesis of magnetite using β-CD may not be as feasible as that using α-CD.

3.10. Effect of Hydrophilic Groups. The clusters of Fe_3O_4 nanoparticles formed at different concentrations of NPE_5 are shown in Figure 11. When [NPE_5] was at 1.5 mM, small irregular clusters of Fe_3O_4 nanoparticles with an average diameter of 25 nm were obtained (Figure 11a). Bigger clusters that were nearly spherical were observed when [NPE_5] was 3 mM and the size was between 40 and 75 nm (Figure 11b). At 6 mM, distinct spherical Fe_3O_4 nanoparticle clusters were formed with a diameter of 80−120 nm (Figure 1b). The clusters formed were mesoporous[36] as compared to those when NPE_9 was used, and were made up of about 500−2000 small Fe_3O_4 nanoparticles with a diameter of about 10 nm. When [NPE_5] was higher than 6 mM, bigger clusters of Fe_3O_4 nanoparticles were formed and excess CD−polymer complex remained (Figure 11c). Hence, using NPE_5 has an effect on both the size and the type of clusters formed.

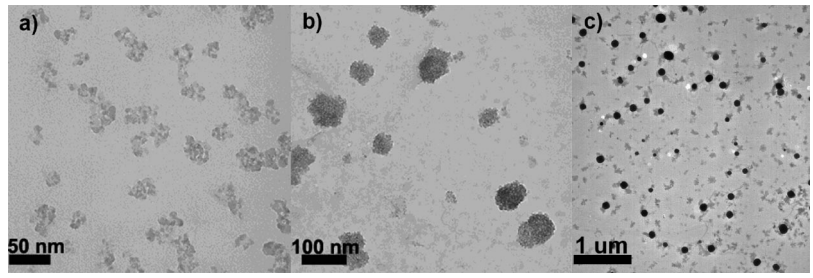

Figure 11. TEM images of Fe_3O_4 clusters at different [NPE_5]: (a) 1.5 mM, (b) 3 mM, and (c) 9 mM ([α-CD] = 2 mM, [Fe^{2+}] = 10 mM, [Fe^{3+}] = 20 mM).

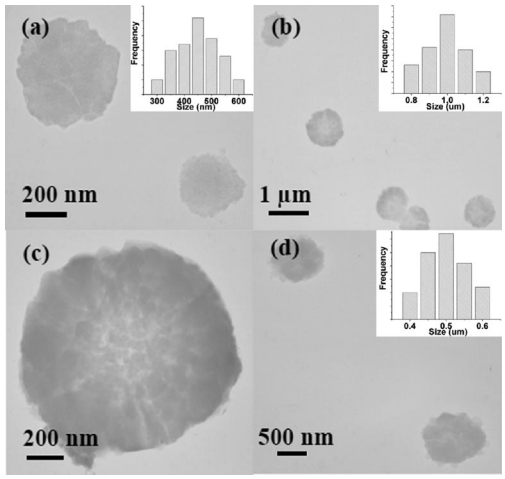

Figure 12. TEM images of Fe_3O_4 clusters at different [NPE_{30}]: (a) 0.43 mM, (b) 0.85 mM, (c) enlargement of (b), and (d) 1.70 mM ([α-CD] = 2 mM, [Fe^{2+}] = 10 mM, [Fe^{3+}] = 20 mM). Insets show histograms of the size distribution of the clusters accordingly.

The TEM images of the Fe_3O_4 nanoparticle clusters formed at different concentrations of NPE_{30} are shown in Figure 12. With NPE_{30}, within the tested range of 0.43−1.75 mM, all the products formed were large, discrete, spherical clusters of Fe_3O_4 nanoparticles and no small dispersed nanoparticles were observed. When the concentration of NPE_{30} was 0.43 mM, the spherical clusters formed were around 330−555 nm in diameter (Figure 12a, inset shows a histogram of the size distribution of the clusters). The size increased to 1 μm (inset shows a histogram of the size distribution of the clusters) when the [NPE_{30}] was 0.85 mM (Figure 12b,c). At 1.75 mM, the clusters decreased to 500 nm (Figure 12d, inset shows a histogram of the size distribution of the clusters). Though there was a change in the size of the Fe_3O_4 nanoparticle clusters formed, the type of clusters formed were unchanged despite the change in the NPE_{30} concentration. Hence, using NPE_{30} has an effect on the size but not the type of clusters formed.

There was a significant increase in size as the number of hydrophilic groups from the surfactants increased. The size range of the clusters formed for NPE_5, NPE_9, and NPE_{30} was from 25 to 120 nm, from 40 to 300 nm, and from 300 to 900 nm, respectively. In addition, the clusters formed using different surfactants were different. The clusters formed with NPE_5 were mesoporous, those formed with NPE_9 were hollow and tightly aggregated, and those formed with NPE_{30} were more solid. It was observed that the density of the clusters was higher as the singular nanoparticles were closer together when the number of hydrophilic groups increased. Therefore, the number of hydrophilic groups will affect the size and density of the clusters formed.

The increase in density and size of the clusters formed may be attributed to the formation of different CD−polymer complexes when different types of polymer surfactants were used. More CDs will thread on the PEG chain (polyethylene glycol (*n*) part) of NPE*n* surfactants while the hydrophilic groups increase from 5, to 9, and then to 30. The number of CDs on the NPE_5, NPE_9, and NPE_{30} is 2, 4, and 15 at initial stage, respectively. Therefore, the CMC of micelles formed by CD−NPE*n* complex will increase and the volume of the micelles will expand. After the formation of an inclusion complex with the hydrophobic groups of the surfactant, the hydroxyl groups of the α-CD rims and the PEG chains can interact themselves.[36,37] This resulted in the possible formation of hydrogen bonding among CDs and between CD and the surfactant. As the number of hydrophilic groups increased, it was likely that these interactions increased because of more CDs threading on the PEG chains of the NPE*n* surfactants. This might lead to linkage or bridging of the surface coating on the nanoparticles and cause singular nanoparticles to cluster together instead of remaining as dispersed nanoparticles and also enhance the interactions between singular nanoparticles, causing them to be more tightly bound together, increasing the density of the clusters. Thus, as the number of hydrophilic groups increased, the number of Fe_3O_4 nanoparticle clusters increased, which were larger and denser while the number of those small dispersed nanoparticles decreased.

The formation mechanism of hollow clusters is proposed as follows. The CD−NPE*n* complex will absorb on the Fe_3O_4 nanoparticles by the hydroxyl groups. The CDs will be added into the solution gradually. Therefore, at the initial stage, the CD concentration will be much lower than the NPE*n* concentration. Hence, the Fe_3O_4 nanoparticles will agglomerate into a dense cluster. When further CDs are added into the solution, only one CD molecule could continue to thread on the PEG chains of NPE_5 (from 1 to 2). The CD will have a smaller effect on the CMC of NPE_5[35] and formed clusters due to small steric effect. The excess CD will bridge the Fe_3O_4 nanoparticles by the absorbed CD on their surfaces by hydrogen bonding. Therefore, the mesoporous clusters of Fe_3O_4 nanoparticles will be formed. Instead of NPE_9, three more CD molecules may continue to thread on the PEG chains of NPE_9 (from 1 to 4) when CDs are added into the solution gradually. The four CD molecules on the PEG chains will have much steric effect. Driven by minimization

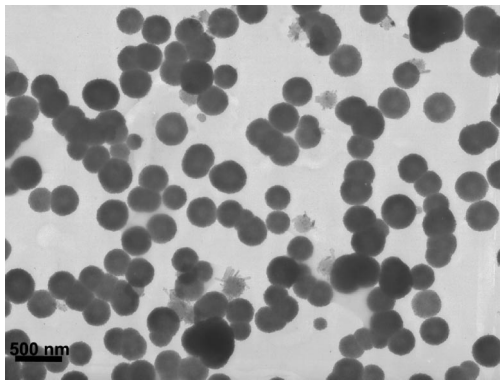

Figure 13. Loose spherical clusters of Fe_3O_4 nanoparticles extracted from the reaction process ([α-CD] = 2 mM, [NPE_9] = 1.75 mM, [Fe^{2+}] = 10 mM, [Fe^{3+}] = 20 mM).

of the total energy of the system, the CD−NPE_9 complexes coated Fe_3O_4 nanoparticles will aggregate together with nondense spherical cluster.[40] The distance between the dispersed Fe_3O_4 nanoparticles will be much bigger, compared with that when NPE_5 is used. The clusters of Fe_3O_4 nanoparticles whose exterior had relatively loose packing will be formed (Figure 13). Moreover, with the reaction continuing, the concentration of the reactants will decrease and the reaction rate will slow down, the exterior Fe_3O_4 nanoparticles packed more loosely than those in the interior of the clusters. Therefore, repacking would occur. The interior Fe_3O_4 nanoparticles will move to the exterior of the clusters to form dense close packing. The surface energy will be reduced by the formation of nearly spherical clusters. Eventually, the hollow clusters of Fe_3O_4 nanoparticles will be formed with increasing reaction time (Figure S1 and Figure 1c). When NPE_{30} is used, 14 more CD molecules will continue to thread on the PEG chains of NPE_9 (from 1 to 14) when CDs are added into the solution at a late stage; however, the actual amount of CDs in the solution is far less than the amount needed. Therefore, the CD addition has little effect on the formed clusters. Due to the strong hydrogen bonding among PEG chains, denser and bigger clusters of Fe_3O_4 nanoparticles were formed. The repacking of Fe_3O_4 nanoparticles also has little effect on the morphology and renders the clusters with small hollow cores.

3.11. Effect of Hydrophobic Groups. Figure 14 shows the clusters of Fe_3O_4 nanoparticles formed at different concentrations of Brij-97. When the concentration of Brij-97 was 0.23 mM, the size of the clusters was about 120 nm (Figure 14a), and when the concentration was increased to 0.45 mM, the size of the spherical clusters increased to about 200 nm (Figure 14b,c, inset shows a histogram of the size distribution of the clusters). At 0.90 mM, clusters of very small nanoparticles were observed (Figure 14d). However, the size of these clusters formed was smaller than the size of the clusters formed with use of NPE_9. Furthermore, the amount of clusters formed with Brij-97 was much lower than that when NPE_9 was used. This is because at least two CDs will thread on the long hydrophobic chain (C_{18}). The CD−surfactant complexes formed less than NPE_9 used at a fixed CD concentration.

With Triton X-114, a cloudy solution was obtained. Upon standing, two layers, aqueous and coacervate layers, were

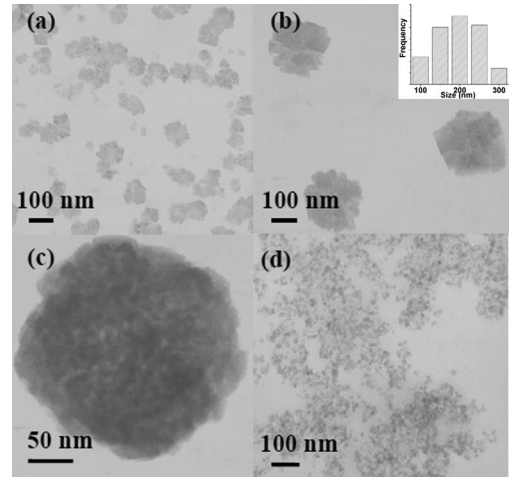

Figure 14. TEM images of Fe_3O_4 clusters at different [Brij-97]: (a) 0.23 mM, (b) 0.45 mM, (c) enlargement of (b), and (d) 0.90 mM ([α-CD] = 2 mM, [Fe^{2+}] = 10 mM, [Fe^{3+}] = 20 mM). Inset shows a histogram of the size distribution of the clusters.

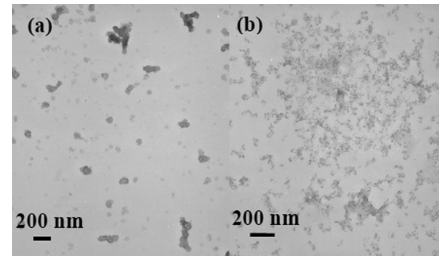

Figure 15. TEM images of Fe_3O_4 clusters at [Triton X-114] = 3.77 mM: (a) top layer and (b) bottom layer ([α-CD] = 2 mM, [Fe^{2+}] = 10 mM, [Fe^{3+}] = 20 mM).

observed (data not shown). When [Triton X-114] was 3.77 mM, TEM images taken from both the top and the bottom layers were shown in Figure 15. It was observed that the amount of the nanoparticles formed in the top water layer was very low. The size range of the clusters was from 125 to 200 nm and the clusters formed were irregular. The bottom layer was found to contain many Fe_3O_4 clusters. The particles formed were small and irregular. This is not surprising as when the surfactant concentration was very high, the formed particles were often small. Hence, it was reasonable to believe that as a type of hydrophobic groups on the surfactant, the solubility of the clusters formed in water will be affected. An inclusion complex was formed between the hydrophobic end of the surfactant and the hydrophobic cavity of the CDs. CD has a rim of hydrophilic groups and hence improved the solubility of Fe_3O_4 nanoparticle clusters in an aqueous solution. When the NPE*n* series was used, no two phases were observed upon standing, unlike the case when Triton X-114 was used. This may be attributed to the difference in binding constants of the two surfactants with α-CD. By Du et al.,[41] a study was carried out on the inclusion complex of several nonionic surfactants with CD. The results showed that CD entrapped the hydrophobic moieties of both the NPE*n* and Triton X-114 to form inclusion complexes. However, unlike the *n*-nonyl group of NPE_9, the *tert*-octyl group of Triton X-114 failed to be effectively encapsulated into the cavity of CD because of the steric hindrance of methyl groups at the rim of the cavity. This was in agreement

with the work reported by Datta and co-workers.[42] This suggested that the formation of the two layers when Triton X-114 was used may be due to the low binding constant of the Triton X-114 with α-CD. Unsuccessful formation of a stable inclusion complex with CD greatly affected the solubility of the clusters formed which were rather insoluble in the aqueous phase. Linear aliphatic groups could also form inclusion complexes with CD, and thus with Brij-97, only one phase was observed.[43]

Considering the results, better water solubility of the Fe_3O_4 nanoparticles should be due to the formation of stable inclusion complexes between the CD and the surfactant. Hence, the type of hydrophobic groups on the surfactant will affect the solubility of the formed complex and further affect the formation of the clusters of Fe_3O_4 nanoparticles.

4. Conclusions

Water-dispersible hollow clusters of Fe_3O_4 nanoparticles have been successfully synthesized in a simple one-step reaction under mild conditions. It was found that the size, morphology, shape, and solubility of the assembled magnetite nanoparticles could be tuned by changing the synthetic parameters such as the concentration of polymer surfactants. In addition, an increase in the number of hydrophilic groups of the surfactants NPE_9 caused the size and density of the Fe_3O_4 nanoparticle clusters to increase compared with those prepared by NPE_5. The structure of the clusters of magnetic nanoparticles can be tuned from mesoporous, to hollow, and to solid by the judicious selection of polymer surfactants. The magnetization of the hollow clusters (114.3 emu g^{-1}) was also comparable to the values of other coated magnetite clusters from other reports. These hollow clusters of Fe_3O_4 nanoparticles have a diameter of about 300 nm and also possess a BET surface area of ca. 141.2 m^2 g^{-1}, which is very important for them as magnetic carriers. Therefore, they also could be used in magnetic separation when properly surface-modified. Currently, to achieve their applications, such as in drug delivery, their mechanic properties are improved by cross-linking them by photopolymerization of one water-soluble monomer. Further studies on their applications are underway.

Acknowledgment. Dr. H. Xia acknowledges the Alexander von Humboldt foundation for a research fellowship. We thank Prof. H. Möhwald and Dr. Dayang Wang for helpful discussion and unknown reviewers for valued comments. The authors are grateful to the Max Planck Society for the financial support and to Shandong University for the start-up funding support.

Supporting Information Available: This material is available free of charge via the Internet at http://pubs.acs.org.

CM900268Z